

**COMBINATION OF OPTICAL METHODS AND ATOMIC FORCE MICROSCOPY
AT CHARACTERIZATION OF THIN FILM SYSTEMS¹****I. Ohlídal^{2*}, D. Franta[†], P. Klapetek[‡]****Department of Physical Electronics, Faculty of Science, Masaryk University,
Kotlářská 2, 611 37 Brno, Czech Republic**†Laboratory of Plasma Physics and Plasma Sources, Faculty of Science, Masaryk University,
Kotlářská 2, 611 37 Brno, Czech Republic**‡Czech Metrology Institute, Okružní 31, 638 00 Brno, Czech Republic*

Received 11 February 2005, accepted 23 February 2005

In this paper the examples of combined analytical methods usable for the characterization of thin film systems are presented. As the optical methods variable angle spectroscopic ellipsometry and spectroscopic reflectometry are used. It is shown that these methods can be employed for the complete determination of both the optical and material parameters of the materials forming the films. Moreover, it is shown that using the combined methods of AFM and the optical methods specified it is also possible to determine the values of the parameters characterizing some defects of the film systems under investigation. Discussion of the reliability of the methods enabling us to determine the values of the statistical quantities describing the boundary roughness of the thin films is also presented. A detailed attention is devoted to the results achieved for these quantities by atomic force microscopy for very finely rough film boundaries (i. e. nanometrically rough boundaries). The practical meaning of the combined methods presented is illustrated using the characterization of several samples of TiO₂ films, hydrogenated polymorphous silicon films and oxide films originating by thermal oxidation of gallium arsenide substrates.

PACS: 68.35.Ct, 68.37.Ps, 95.75.Fg

1 Introduction

Thin film systems are frequently employed in practice. In particular these systems play an important role in various branches of both the applied research and industry. For example, they are utilized as interference devices in optics industry, wave-guides in optoelectronic, important elements in electronic and semiconductor industries etc. In many practical applications the optical properties of the thin film systems are very important. Therefore it is necessary to have reliable and efficient methods enabling us to characterize the optical properties of these systems. So far

¹Presented at SSSI-IV (Solid State Surfaces and Interfaces IV) Conference, Smolenice, Slovakia, 8–11 Nov. 2004.²E-mail address: ohlidal@physics.muni.cz

many optical methods have been developed for this purpose. From the practical point of view the analytical methods employing ellipsometry and spectrophotometry are the most significant ones. Using these methods one can namely perform the optical characterization of the majority of the thin film systems completely, i. e. the values of all the parameters describing these systems unambiguously from the optical point of view can be determined using these methods.

The optical properties of the thin film systems are dependent on their structure. That is why the optical methods used to characterize the optical properties of these systems must often be combined with the methods enabling us to study their structure. For example, the optical methods are combined with various X-ray methods, electron beam methods, ion beam methods etc. During the two last decades the optical methods were also combined with atomic force microscopy (AFM) and the other techniques of scanning probe microscopy.

In this paper some examples of the methods employing the combination of the ellipsometric and spectrophotometric methods with AFM enabling us to perform the complete optical analysis miscellaneous layered systems taking place in practice will be presented.

2 Descriptions of the methods

In this section the brief descriptions of the most employed ellipsometric and spectrophotometric methods usable for the characterization of the optical properties of the thin film systems will be presented. Moreover, the role of AFM will be discussed in optical studies of these systems as well.

2.1 Ellipsometric methods

The ellipsometric methods are based on measuring and interpreting the ellipsometric quantities (e. g. ellipsometric parameters) describing the polarization states of light reflected or transmitted by the thin film systems under investigation (see Refs. [1–3]). These ellipsometric methods can be divided into the two basic groups:

1. methods of monochromatic ellipsometry
2. methods of spectroscopic ellipsometry.

Within the monochromatic ellipsometric methods the ellipsometric quantities of the systems characterized are measured as the functions of the angle of incidence or refractive index of the ambient for one wavelength selected. The methods of spectroscopic ellipsometry are based on the measurements of the ellipsometric quantities within spectral regions of interest. The detailed classification and description of the methods belonging to both the groups are presented in Refs. [1, 2].

At present the methods of spectroscopic ellipsometry are mainly used to characterize the thin film systems in practice since these methods give more detailed information concerning the optical properties of these systems than the methods of monochromatic ellipsometry. The most popular method of spectroscopic ellipsometry is variable angle spectroscopic ellipsometry (VASE). Within this method the spectral dependences of the ellipsometric quantities of the systems are measured for several angles of incidence within the spectral region of interest (see e. g. Ref. [2]). The ellipsometric quantities of the systems are usually measured in air so that from

the mathematical point of view the ellipsometric quantities corresponding to VASE are the functions of two variables, i. e. wavelength and incidence angle, that can be varied independently at measuring these quantities using the experimental arrangements called ellipsometers. Reviews of the various types of the ellipsometers usable for measurements of the different ellipsometric quantities of the systems investigated are presented, for example, in Refs. [1, 2].

The VASE experimental data of the samples analyzed are treated using miscellaneous numerical procedures. The least-squares method (LSM) belongs to the numerical methods mostly employed in optical studies of the layered systems in practice. Within the LSM various merit functions can be employed. For example, the following merit function can be used to treat the experimental data corresponding to VASE:

$$S(\vec{X}) = \sum_{i=1}^N |\hat{\rho}_i^{\text{EXP}} - \hat{\rho}(\lambda_i, \theta_{0i}, \vec{X})^{\text{TEOR}}|^2 w_i, \quad (1)$$

where the summation is performed over all the experimental values of the ellipsometric ratio $\hat{\rho}$ ($\hat{\rho} = \hat{r}_p/\hat{r}_s = \tan \Psi \exp(i\Delta)$, where \hat{r}_p , \hat{r}_s , Ψ and Δ denote the reflection Fresnel coefficient for the p-polarization, reflection Fresnel coefficient for the s-polarization, azimuth and phase change of the system, respectively) and $\hat{\rho}_i^{\text{EXP}}$ is the ellipsometric ratio measured for a certain value of the wavelength λ_i and certain angle of incidence θ_{0i} . The weights of the experimental data are denoted by symbol w_i . The theoretical values of the ellipsometric ratio are represented by symbol $\hat{\rho}(\lambda_i, \theta_{0i}, \vec{X})^{\text{TEOR}}$, where vector \vec{X} represents the optical parameters sought for the thin film system analyzed. These theoretical values are calculated using formulae belonging to the individual thin film systems. The matrix formalism is mostly used to derive these formulae (see e. g. Refs [2, 4]). Of course, the concrete formulae for $\hat{\rho}(\lambda_i, \theta_{0i}, \vec{X})^{\text{TEOR}}$ must be derived on the basis of both the structural and dispersion models corresponding to the thin film system characterized (see below). In practice the multi-sample modification of VASE can be employed to carry out the optical characterization of the thin films and their systems. Within the framework of this modification the experimental data of several samples of the system studied are simultaneously treated. The samples used for such the characterization must mutually differ in values of one or more parameters while the values of the remaining parameters must be identical. For example, the samples can mutually differ in values of the thicknesses and the values of the remaining parameters characterizing these samples such the optical constants are the same. The multi-sample modification of VASE is described in detail in our earlier papers [5–7].

2.2 Spectrophotometric methods

The spectrophotometric methods are based on interpreting the spectral dependences of the reflectances or transmittances measured within certain spectral regions. In principle these reflectances and transmittances can be measured at the oblique incidence but the spectrophotometric methods employing the spectral dependences of the reflectance or transmittance measured at near-normal or normal incidence, respectively, are mostly utilized in practice. In this case the following merit function can be used to treat the spectrophotometric experimental data by the LSM:

$$S(\vec{X}) = \sum_{i=1}^N [P_i^{\text{EXP}} - P(\lambda_i, \theta_{0i}, \vec{X})^{\text{TEOR}}]^2 w_i, \quad (2)$$

where P denotes the reflectance or transmittance. i. e. $P = R = |\hat{r}|^2$ or $P = \tau = \frac{n}{n_0}|\hat{t}|^2$. Symbols R , \hat{r} , τ and \hat{t} are the reflectance, reflection Fresnel coefficient, transmittance and transmission Fresnel coefficient of the layered system, respectively. Symbols n and n_0 denote the refractive indices of the non-absorbing substrate of the system and ambient, respectively. The concrete formulae for calculating the theoretical values of \hat{r} and \hat{t} are again given by the structural and dispersion models of the thin film systems and they can also be derived using the matrix formalism.

Note that VASE and spectroscopic methods can be combined. Within this optical combined method the ellipsometric and spectrophotometric experimental data are treated simultaneously for one or several samples of the layered system under study (for details see Refs. [2, 8, 9]). It should also be noted that the transmittance data of the systems can only be measured if the substrates are non-absorbing.

2.3 Atomic force microscopy

AFM is one of significant methods for observation and investigation of surface morphology of solids (see e. g. Refs. [10, 11]). This experimental technique has also been employed for the structural analysis of the boundaries of various thin film systems [12–15]. In particular statistical roughness of the thin film boundaries can be studied by AFM precisely and exactly. Using the AFM analysis one can determine the values of the statistical quantities such as the rms value of the heights and power spectral density function of the boundary roughness irregularities influencing the ellipsometric and spectrophotometric quantities employed for the characterization of the optical properties of the layered systems studied [13–15]. Strictly speaking the AFM analysis of the thin film boundaries enables us to evaluate the values of the statistical quantities taking place in the formulae expressing the optical quantities used to characterize the optical properties of the layered objects studied. Thus, the AFM analysis of the boundary roughness can be used as the method enabling us to check or complete the results of the optical characterization of these systems. The AFM measurements can be realized in several modes from which the contact mode, non-contact mode and tapping mode are the most relevant from the practical point of view. In detail the specifications of these modes are presented, for example, in Ref. [16]. However, there are certain difficulties connected with using AFM as the auxiliary method in the optical analysis the thin films and their systems. Therefore, it is necessary to be very careful in using AFM at the optical characterization of the layered systems (see below).

3 Models of the thin film systems

As mentioned above the physical models of the thin film systems studied must be employed for deriving the formulae expressing the individual optical quantities of these systems to be used to treat the corresponding experimental data. In principle it is necessary to have the models representing the structure of the systems and the dispersion models, i. e. the models expressing the spectral dependences of the optical constants of the thin films of the systems within corresponding spectral regions.

The structural models express the composition of the systems, i. e. the sequence of the individual films owing to the substrate. Furthermore, this model expresses the following assumptions:

1. Assumption concerning the properties of the materials forming the individual films and substrate (i. e. it contains information whether the film materials are optically homogeneous, inhomogeneous, isotropic, anisotropic etc.)
2. Assumption concerning the structure of the boundaries between the individual films (e. g. whether the boundaries are smooth or rough, information about the structural model of boundary roughness etc.)
3. Assumption concerning volume defects inside the films and substrate (e. g. the assumption expressing the existence of voids and pores inside them etc.)
4. Assumption concerning information about the optical properties of the ambient (the ambient mostly consists of air or non-absorbing liquids).

The dispersion models of the optical constants of the materials forming the individual films, i. e. the refractive indices and extinction coefficients, are empirical ones. They are mostly based on parameterization of the optical constants or the complex dielectric function (there are unambiguous mathematical formulae between the optical constants on the one hand and the dielectric function on the other hand). Within this parameterization the optical constants or dielectric function are expressed as functions of the wavelength that contain some material parameters. For example, for slightly absorbing materials the refractive index n and extinction coefficient k can be described by the Cauchy's formula and exponential formula, respectively, within the corresponding spectral range, i. e.

$$n = A + \frac{B}{\lambda^2} \quad (\text{Cauchy's formula}) \quad (3)$$

and

$$k = a \exp(-b\lambda) \quad (\text{exponential formula}), \quad (4)$$

where A , B , a and b are the material parameters.

Of course, the dispersion models can be based on parameterization of the quantities connected with the electron band structure of the materials of the films too. For example, the dispersion models can be based on parameterization of the density of electronic states (DOS) (see e. g. [8]). In this case the DOS is expressed as a function of the wavelength or photon energy containing the material parameters such as the band gap.

It should be noted that some of the methods of the optical characterization of the thin film systems do not need the dispersion models. Within the framework of these methods the values of the parameters describing the system analyzed including the optical constants are determined for individual selected wavelengths corresponding to spectral region of interest (see e. g. [2, 17]). These methods are called the single-wavelength methods. Within these methods the spectral dependences of the optical constants of the films are determined without postulating some spectral function parameterized representing the spectral dependences of these quantities. The physical interpretation of the spectral dependences of the optical constants can then be performed in the following step of the analysis of the systems.

4 Examples of the combined methods

In this section the examples of the useful methods for the optical characterization of the thin films and their systems based on combination of VASE, spectrophotometry and AFM will be presented. These methods can be classified into the two basic groups. The first group is formed by the methods in which AFM serves as the method checking the values of the structural parameters (e. g. the rms value of the heights of the boundary roughness irregularities) determined together with the optical and material parameters by means of the optical methods. These methods will be called the combined methods with the AFM checking (the abbreviation CM1 will be used to denote these methods). The latter group is formed by the methods in which the values of the structural parameters determined using AFM are taken as the known and fixed parameters for the optical analysis of the systems by means of which the optical and material parameters are only evaluated. These methods will be called the combined methods with the active role of AFM (the abbreviation CM2 will be used to denote these methods).

4.1 Combined methods with AFM checking (CM1)

The typical example of the CM1 is the method used to perform the complete optical characterization of TiO₂ (titania) thin films prepared onto silicon single crystal substrates by reactive vacuum evaporation using an electron gun (see our earlier paper [6]). The optical method corresponding to the multi-sample modification of the method based on combining VASE and near-normal spectroscopic reflectometry (NNSR) was utilized for determining the values of the optical parameters and structural quantities describing the titania films studied (it was assumed that the individual titania films exhibited the same optical constants while the remaining parameters were different). This means that the following merit function was employed for treating the experimental data corresponding to this optical method:

$$S(\vec{X}) = \sum |\hat{\rho}_{ij}^{\text{EXP}} - \hat{\rho}_{ij}^{\text{TEOR}}(\lambda, \theta_0, \vec{X})|^2 w, \quad (5)$$

where the summation is performed over all the experimental values of the optical data used. Symbol $\hat{\rho}_{ij}^{\text{EXP}}$ denotes the experimental data of the ellipsometric quantities and relative reflectance, defined as follows

$$\hat{\rho}_{ii}^{\text{EXP}} = \tan \Psi_i \exp(i\Delta_i), \quad \text{for } i = j, \quad (6)$$

$$\hat{\rho}_{ij}^{\text{EXP}} = \frac{R_i}{R_j} + i \frac{R_j}{R_i}, \quad \text{for } i \neq j. \quad (7)$$

Symbols Ψ_i and Δ_i denote the ellipsometric parameters corresponding to the i -th sample for certain value of the incidence angle θ_0 and wavelength λ . Symbols R_i and R_j represent the reflectance of the j -th and i -th sample, respectively. The remaining symbols have the same meaning as before.

The optical characterization was carried out within the spectral region 220–850 nm (VASE was applied for five incidence angles in the interval 55–75°). In this paper it was shown that the two defects had to be considered in the structural model of the titania films studied, i. e. slight statistical roughness of the upper boundaries and optical inhomogeneity of the films consisting

Tab. 1. The values of the thicknesses d_i and statistical parameters of the upper boundaries of the titania films σ_i and T_i determined by both the optical and AFM data fits (d_i , σ_i and T_i denote the thickness, rms value of the heights and autocorrelation length of the i -th sample, respectively).

sample no.	optical data fit			AFM data fit	
	d_i [nm]	σ_i [nm]	T_i [nm]	σ_i [nm]	T_i [nm]
1	49.17 ± 0.01	2.59 ± 0.03	10.2 ± 0.3	0.266 ± 0.001	9.1 ± 0.1
2	146.29 ± 0.01	2.66 ± 0.04	11.8 ± 0.5	0.443 ± 0.002	11.1 ± 0.1
3	294.52 ± 0.01	3.24 ± 0.04	11.5 ± 0.3	1.333 ± 0.013	23.0 ± 0.5
4	636.91 ± 0.02	6.01 ± 0.04	22.8 ± 0.4	1.925 ± 0.022	63.0 ± 1.7
5	986.31 ± 0.03	8.50 ± 0.04	28.0 ± 0.4	4.100 ± 0.047	93.2 ± 2.6

in the continuous profile of the complex refractive index across these films. Both the defects mentioned above were caused with the columnar structure of the titania films (for details see paper [6]). The complex refractive index profile $n(z)$ of the titania films was represented by the following function:

$$\hat{n}^2(z) = p(z) \hat{n}_R^2 + [1 - p(z)] \hat{n}_\infty^2, \quad (8)$$

$$p(z) = \exp[(z - d)/b]. \quad (9)$$

where symbols \hat{n}_R , \hat{n}_∞ , b and d denote the complex refractive index of the TiO_2 film adjacent to the boundary between the substrate and film, the asymptotic complex refractive index of the titania film (i. e. in practice this refractive index corresponds to the ambient boundary of a very thick film), the parameter expressing the rate of change of the refractive index and the thickness of the film, respectively. The influence of the boundary roughness on the ellipsometric quantities and reflectance was respected using the Rayleigh-Rice theory (RRT) [18]. Using the optical method utilized the values of d , b , σ and T were determined for all the films studied. Symbols σ and T denote the rms value of the heights and autocorrelation length of the upper boundary (σ and T are the parameters of the power spectral density function (PSDF) taking place in the formulae corresponding to the RRT). Moreover, using this method the values of \hat{n}_R and \hat{n}_∞ were determined at all the wavelengths selected in the spectral region of interest. In Fig. 1 the spectral dependences of the real and imaginary parts of the complex dielectric function determined for the inhomogeneous titania films corresponding to the film/substrate boundary ($\hat{\epsilon}_R = \hat{n}_R^2$) and the ambient/film boundary corresponding to very thick film ($\hat{\epsilon}_\infty = \hat{n}_\infty^2$) are presented. The values of the thickness and roughness parameters determined using this optical method for the individual samples are summarized in Table 1. Moreover, in this table the values of the roughness parameters determined using AFM are introduced for the same samples. The values of σ and T were determined by fitting the PSDFs measured for the upper boundaries of the titania films using the method described in detail in papers [13–15]. This means that the PSDF experimental data measured by AFM were fitted using the following formula:

$$W_1(K) = \frac{\sigma^2 T}{2\sqrt{\pi}} e^{-(KT/2)^2}, \quad (10)$$

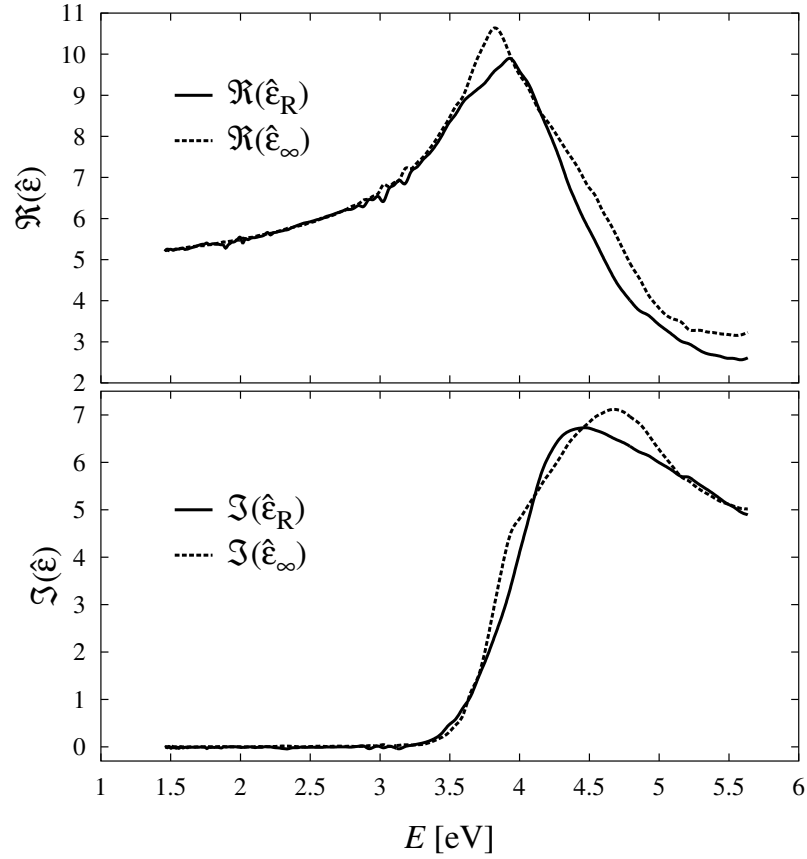


Fig. 1. The spectral dependences of the real and imaginary parts of the dielectric function of the titania films for the substrate boundary ($\hat{\epsilon}_R = \hat{n}_R^2$) and for the ambient boundary corresponding to the very thick film ($\hat{\epsilon}_\infty = \hat{n}_\infty^2$). Symbol \Re and/or \Im denotes the real and/or imaginary part of the corresponding quantity.

where K_x denotes the components of the wavevectors of the harmonic components of the boundary roughness. The fit of the PSDF data found using AFM is shown in Fig. 2. The experimental AFM data in Fig. 2 correspond to the AFM scan obtained for sample no. 5 (see Fig. 3). From Table 1 one can see that there are considerable differences between the values of the statistical parameters of roughness determined by AFM and by the combined optical method of VASE and NNSR. The same conclusion is true for the PSDFs determined using AFM and the optical methods (see Fig. 2). In our opinion there were three main reasons for this:

1. The components of surface roughness with spatial wavelengths (lateral dimensions) smaller than the diameter of the AFM tip are suppressed within AFM measurements, i. e. they are smoothed (for details see below).
2. Within our optical method the existence of surface layers on the upper boundaries of the

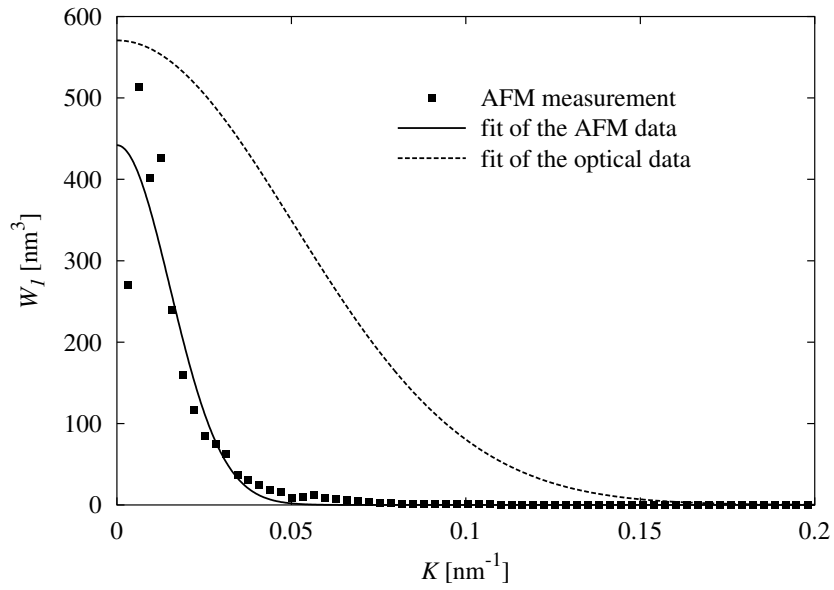


Fig. 2. The PSDF of sample no. 5: the points represent PSDF determined by AFM; full line represents AFM data fit; dashed line represents corresponding PSDF function determined by the optical data fit.

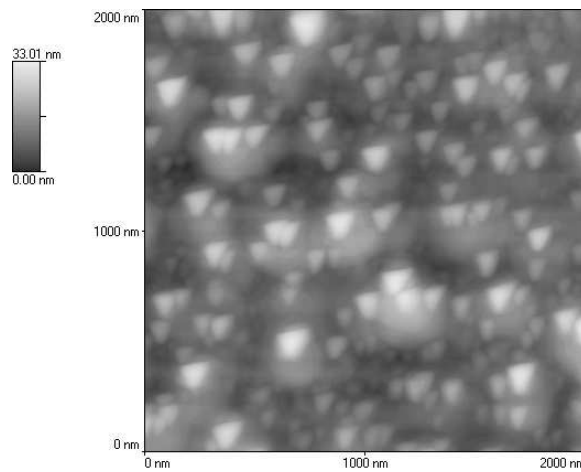


Fig. 3. The image of the part of the upper boundary of sample no. 5. The condition of the AFM measurements: non-contact mode; scanned area $2 \times 2 \mu\text{m}$ (400×400 pixels); tube scanner; standard non-contact tip; scan rate $3 \mu\text{m/s}$.

TiO₂ thin films originating from adsorption gases (H₂O, CO₂ etc.) was not considered because these layers were extremely thin.

3. Within the optical model the PSDFs of the upper boundaries were assumed in the form of a Gaussian function. Of course, this assumption need not be fulfilled strictly.

Using the parameter values taking place in Eqs. (8) and (9) one can easily calculate the profiles of the refractive index and extinction coefficient of the titania films for every wavelength. It should be noted that the method employed for characterizing the titania films belongs to the CM1 that does not need to use the dispersion model of the film studied.

The same combined method was used to characterize rough hydrogenated polymorphous silicon films (pm-Si:H) prepared onto silicon single substrates in a capacitively coupled RF glow discharged system by the decomposition of a 3% silane-in-hydrogen gas mixture under RF power of 100 mW/cm² [8]. However, within this method the dispersion model of the optical constants of these films were employed in contradiction with the method utilized for characterizing the TiO₂ films.

This dispersion model is based on parameterization of the DOS. The DOS distribution of the valence and conduction bands $N_{v,c}(E)$ is then expressed as follows [19]:

$$N_{v,c}(E) = \begin{cases} A(E) \sqrt{|E| - \frac{E_g}{2}} \sqrt{\frac{E_h}{2} - |E|}, & \frac{E_g}{2} < |E| < \frac{E_h}{2} \\ 0, & \text{otherwise.} \end{cases} \quad (11)$$

where E is photon energy, E_g and E_h are the band gap and maximum of energy of the interband transitions (for details see [19]). The quantity $A(E)$ is proportional to the valence electron density of the material. The contribution of the interband transitions to the imaginary part of the dielectric function is given by the following convolution [20]:

$$\varepsilon_{2,vc}(E) = \left(\frac{2\pi e\hbar}{mE} \right)^2 \frac{(2\pi)^3}{2} \frac{1}{B_0} |p_{vc}|^2 \int_{-\infty}^{\infty} N_v(S) N_c(S + E) dS, \quad (12)$$

where e , \hbar , m , B_0 and $|p_{vc}|^2$ are electronic charge, Planck's constant, electronic mass, certain part of the Brillouin zone of the corresponding crystalline material and squared momentum-matrix element, respectively. Function $A(E)$ is expressed in this way

$$A(E) = A \left\{ 1 + A_0 \exp \left[-\frac{(|E| - \frac{E_0}{2})^2}{2B_0^2} \right] \right\}. \quad (13)$$

Where A , A_0 , B_0 and E_0 are the parameters.

The DOS distribution corresponding to the localized states exhibits the exponential form [21]:

$$N_1(E) = \begin{cases} AA_1 \exp\left(\frac{|E| - \frac{E_m}{2}}{E_1}\right), & |E| < \frac{E_m}{2} \\ 0, & \text{otherwise.} \end{cases} \quad (14)$$

where A_1 and E_m are again the material parameters. The contribution of the transitions between the occupied localized states and non-occupied extended states taking place in the conduction

band to the dielectric function is expressed as follows:

$$\varepsilon_{2,lc}(E) = \frac{1}{E^2} \int_{-\infty}^{E_F=0} N_1(S) N_c(S + E) dS. \quad (15)$$

where E_F is the Fermi energy. Similarly the contribution of the transition between the occupied extended states taking place in the valence band and non-occupied localized states to the dielectric function is expressed as:

$$\varepsilon_{2,vl}(E) = \frac{1}{E^2} \int_{E_F=0}^{\infty} N_v(S - E) N_1(S) dS. \quad (16)$$

One can see that the foregoing two integrals are identical.

The resulting the dielectric function of the material of the pm-Si:H films is then given by the following formula:

$$\varepsilon_2(E) = \frac{1}{E^2} \int_{-\infty}^{E_F=0} [N_v(S) + 2N_1(S)] N_c(S + E) dS. \quad (17)$$

The real part of the dielectric function was calculated numerically by means of the Kramers-Kronig relation [19]. Thus, the dispersion model used to characterize of the pm-Si:H films contained 9 parameters sought. Within the structural model of the pm-Si:H the following defects of these films were considered: slight statistical roughness of the upper boundaries, overlayers on the upper boundaries and transition layers (TL) between the substrates and pm-Si:H films. The boundary roughness was again included by means of the RRT into the formulas expressing the optical quantities. For including the TL into calculation the Drude approximation was used [2, 4]. The overlayers were represented with very thin films with the refractive index fixed in values corresponding to amorphous SiO₂. The formulae for the ellipsometric quantities and reflectances of the pm-Si:H/Si system were again derived using the matrix formalism and the LSM was employed for treating the experimental data. The values of the roughness parameters determined using the optical method and AFM are summarized in Table 2. One can again see evident differences between the values of these roughness parameters found by both the mentioned methods. By means of the values of the evaluated material parameters taking place in the formulae expressing the dispersion model of the films studied the DOS distribution of the pm-Si:H films were calculated (see Fig. 4).

The spectral dependences of the optical constants of the pm-Si:H films corresponding to the DOS found are plotted in Fig. 5. For comparison the spectral dependences of the optical constants of silicon single crystal (see [22]) and transition layers are also introduced in this figure.

The illustration of the agreement between the experimental data and the theoretical ones calculated on the basis of the values of the parameters found using the LSM is introduced in Fig. 6. The agreement between these data is excellent. Note the values of thickness of the individual pm-Si:H films were determined in the following values: 26.5, 63.5, 190.5, 371.8 and 1246 nm.

The value of the overlayer thickness was assumed to be identical for all the samples of the pm-Si:H films and it was determined in value of 1.93 nm. The methods belonging to CM1 were employed in many other articles such as in [5, 9, 23, 24].

Tab. 2. The values of the roughness parameters of the pm-Si:H films studied to be determined using AFM and optical method.

Reference	AFM		optical method	
	σ [nm]	T [nm]	σ [nm]	T [nm]
005045	0.115	38.5	0.2	33.6
005044	0.187	38.1	0.431	33.6
005034	0.376	35.1	0.628	33.6
005043	0.501	50.5	2.216	30.9
005091	1.164	55.0	3.082	28.9

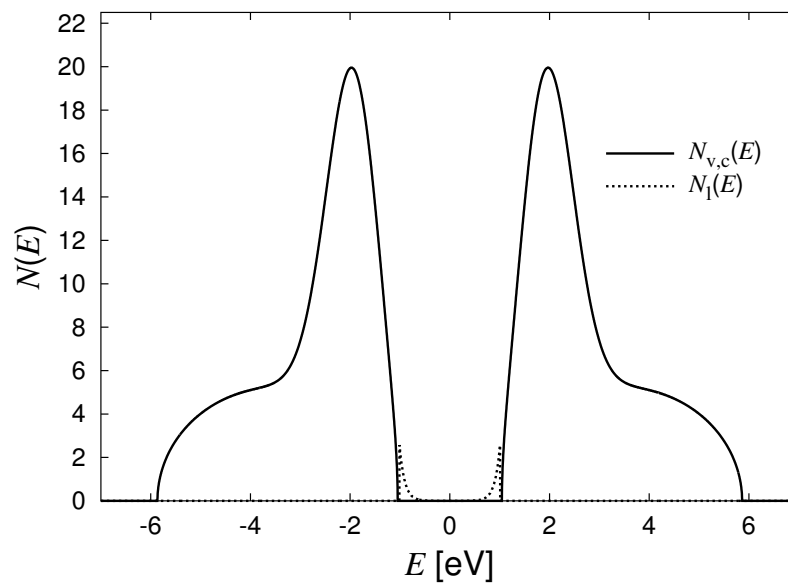


Fig. 4. The unnormalized DOS distribution of the pm-Si:H film studied to be calculated using the nine-parameter dispersion model. Symbols $N_{v,c}(E)$ and $N_1(E)$ denote the unnormalized DOS distribution of the extended and localized states, respectively.

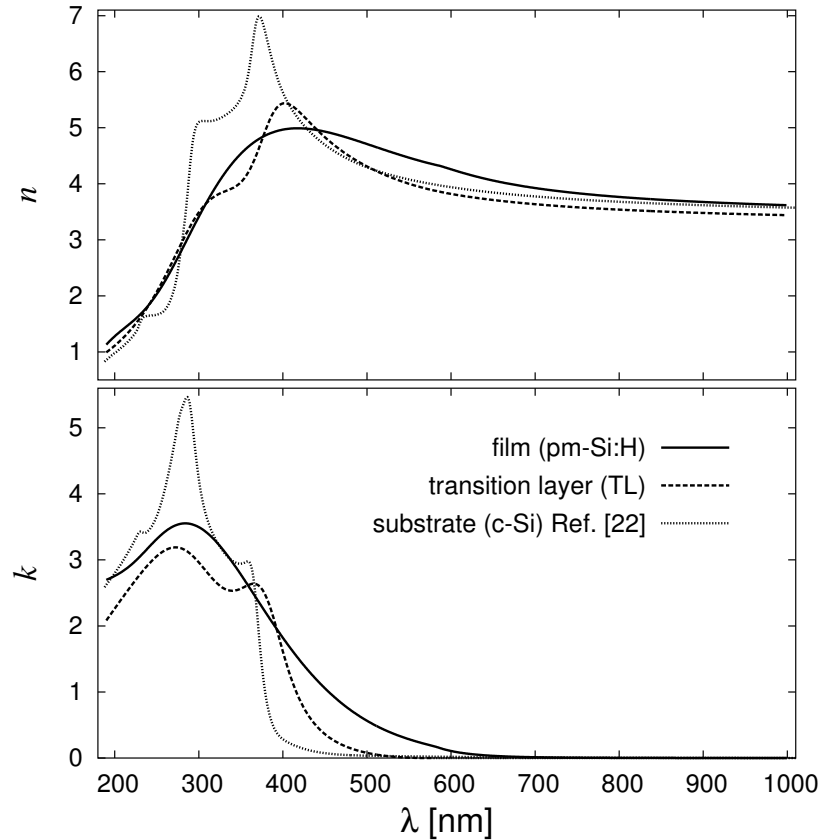


Fig. 5. The spectral dependences of the refractive index n and extinction coefficient k of the pm-Si:H films, TL and c-Si substrates.

4.2 Combined methods with including AFM (CM2)

For the optical characterization of some layered systems it is necessary to determine a great number of parameters. Sometimes these parameters can be correlated mutually. In this case one cannot determine the values of all the parameters unambiguously. Then it is necessary to evaluate some of the parameters sought by auxiliary methods in an independent way. In many cases of the optical characterization of the complicated layered systems AFM can be the efficient auxiliary method enabling us to reduce the number of the parameters sought and perform the complete reliable characterization of these systems.

The typical example of the method belonging to the CM2 is the method employed for characterizing thermal oxide films on GaAs single crystal substrates presented in paper [25]. The oxide thin films originating by thermal oxidation of the surfaces of GaAs single crystals exhibit very complicated structure and chemical composition. Therefore the optical characterization of

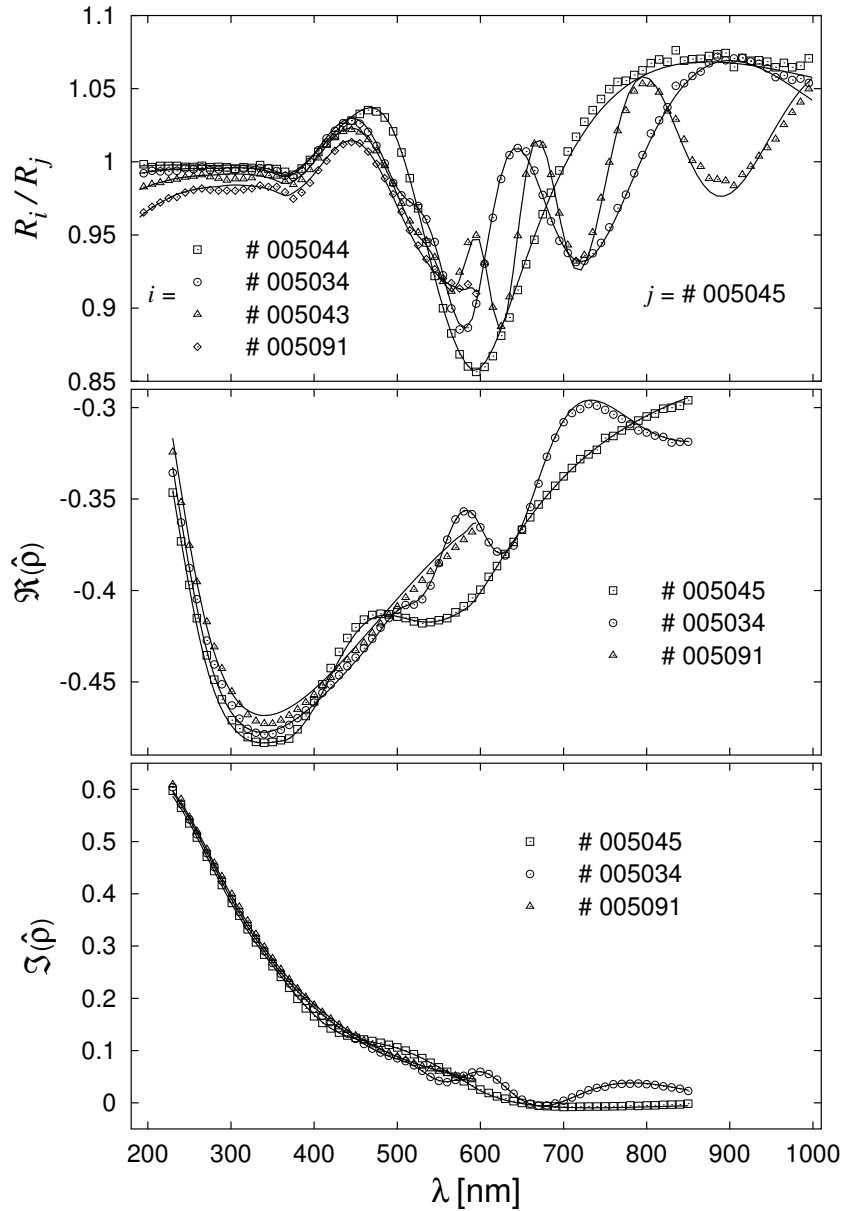


Fig. 6. The spectral dependences of the relative reflectance R_i/R_j , real part of the ellipsometric ratio $\Re(\hat{\rho})$ and imaginary part of the ellipsometric ratio $\Im(\hat{\rho})$ of the selected pm-Si:H films: curves and/or points denote the theoretical and/or experimental data (the ellipsometric dependences correspond to one of the incidence angles used, i. e. to 65°).

these films is very difficult. In paper [25] the multi-sample modification of the combined method of VASE and NNSR was used to analyze the thermal oxide films created on the GaAs surfaces at the temperature of 500 °C in air. This analysis was carried out within the near-UV and visible regions. In the structural model of these films the following defects were taken into account: statistical roughness of both the upper and lower boundaries and optical inhomogeneity corresponding to the relatively complicated profile of the complex refractive index across the films. In the formulae for the optical quantities of the system formed by oxide film/GaAs substrate derived using the matrix formalism the boundary roughness was respected by the RRT. It was assumed that the films were sufficiently thick so that the cross-correlation effects could be neglected. This assumption implies that for expressing the optical quantities of the rough films the approximation presented in [2] can be employed. Within this approximation all the rough boundaries of the layered system are represented with individual matrices. The individual boundary matrix contains the eight Fresnel coefficients calculated numerically. For example, the Fresnel reflection coefficient corresponding to the right-going p-polarized wave incident on the boundary from the left side is expressed as follows:

$$\hat{r}_{\text{pR}} = \hat{r}_{\text{pR}}^{(0)} + \sigma^2 \iint_{-\infty}^{\infty} \hat{f}_{\text{pR}}(K_x, K_y) w(K_x - n_0 k_0 \sin \theta_0, K_y) dK_x dK_y, \quad (18)$$

where $\hat{r}_{\text{pR}}^{(0)}$ is the corresponding Fresnel coefficient of the smooth boundary, w represents the normalized PSDF and \hat{f}_{pR} is the function of the optical constants of the system, incidence angle and wavelength. Furthermore, $k_0 = 2\pi/\lambda$ is the wavenumber and K_x and K_y are components of the wavevectors of the harmonic components of the boundary roughness. The profile of the refractive index of the oxide films was represented by the following function:

$$\hat{n}(z) = \sqrt{\hat{\varepsilon}_{\text{R}} + [(\hat{\varepsilon}_{\text{R}} - 1)p + 1 - \hat{\varepsilon}_{\text{R}}]q(z)}, \quad (19)$$

where $\hat{\varepsilon}_{\text{R}}$ is the dielectric function of the material forming the film at the right boundary (oxide/substrate). Function $q(z)$ is equal zero for z smaller than a certain value z_1 and $q(z)$ is equal to unity for z greater than a certain value z_2 . Within the interval $z_1 < z < z_2$ function $q(z)$ is linear. Symbol p denotes the parameter determining the value of the dielectric function at the left boundary (air/oxide film boundary). The dielectric function $\hat{\varepsilon}_{\text{R}}$ was again given by the dispersion model based on the DOS parameterization. For treating the ellipsometric and reflectometric data the LSM was again utilized. The values of all the parameters corresponding to the physical model of the oxide films could not be determined because of their mutual correlation. Therefore the values of the autocorrelation length T were fixed for all the samples studied in the values found using AFM by fitting the PSDF. After this fixing the values of the remaining parameters describing all the oxide films could be determined unambiguously by using the optical method employed. The values roughness parameters, thicknesses and parameters describing the refractive index profile are introduced for two oxide films on GaAs in Table 3. In this table two thicknesses for each film are presented, i. e. d_{fR} and d_{fE} . Symbols d_{fR} and d_{fE} denote the film thicknesses corresponding to the reflectometric and ellipsometric data. Some oxide films exhibit a small degree of thickness non-uniformity that was respected by assuming the different values of the film thickness for the samples studied (this assumption is reasonable because the light

Tab. 3. The values of the parameters characterizing the thermal oxide films on GaAs studied to be determined using AFM and optical method. Indices 1 and 2 correspond to the upper and lower boundaries, respectively.

method	parameter	sample	
		#2	#3
AFM	σ_1 [nm]	1.93	1.75
	T_1 [nm]	456	414
	σ_2 [nm]	28.5	22.1
	T_2 [nm]	655	531
optical	σ_2 [nm]	25.5	23.4
	d_{fE} [nm]	493	418
	d_{fR} [nm]	487	418
	z_1/d_f	0.782	0.760
	z_2/d_f	0.915	0.937
	p	1.63	1.18

spots on the films under investigation were mutually different in ellipsometric and reflectometric measurements). From Table 3 it is evident that one oxide film exhibited the certain thickness non-uniformity while the latter one was uniform in thickness. Symbol d_f introduced in Table 3 denotes the mean value of both the thicknesses d_{fR} and d_{fE} . The spectral dependences of the refractive index and extinction coefficient of the oxide films corresponding to the boundary oxide film/substrate calculated on the basis of the dispersion parameter values found using the optical method are plotted in Fig. 7. In this figure the spectral dependence of the refractive index of the oxide films studied in paper [26] is plotted for comparison (the conditions of preparing the oxide films studied in paper [26] were identical with those used in paper [25]). From Table 3 is also seen that for the oxide films characterized the lower boundaries are much more rougher than the upper boundaries. This fact was confirmed by the AFM measurements which is illustrated in Fig. 8. In this figure the AFM scans of both the boundaries of one of the oxide films are presented (sample No 2, see Table 3). Note that the AFM scans of the lower boundaries were obtained after dissolution of the oxide films (for details see paper [25]). Moreover, it should be noted that PSDF and one-dimensional distribution of the heights of the lower boundaries of the oxide films were identical with the corresponding Gaussian functions. In Figs. 9 and 10 this fact is illustrated for the lower boundary of the other sample of the oxide film. From the foregoing it is thus apparent that AFM can serve as very helpful auxiliary analytical method at the optical characterization of the thin films exhibiting the complicated structure from the physical point of view. However, similarly as for the methods belonging to the CM1 it is necessary to apply AFM very carefully within the CM2 (see the following section).

5 Discussion

From the examples of combining the optical methods and AFM at the optical characterization of the thin film systems it is clear that AFM can be very useful method for determination of the

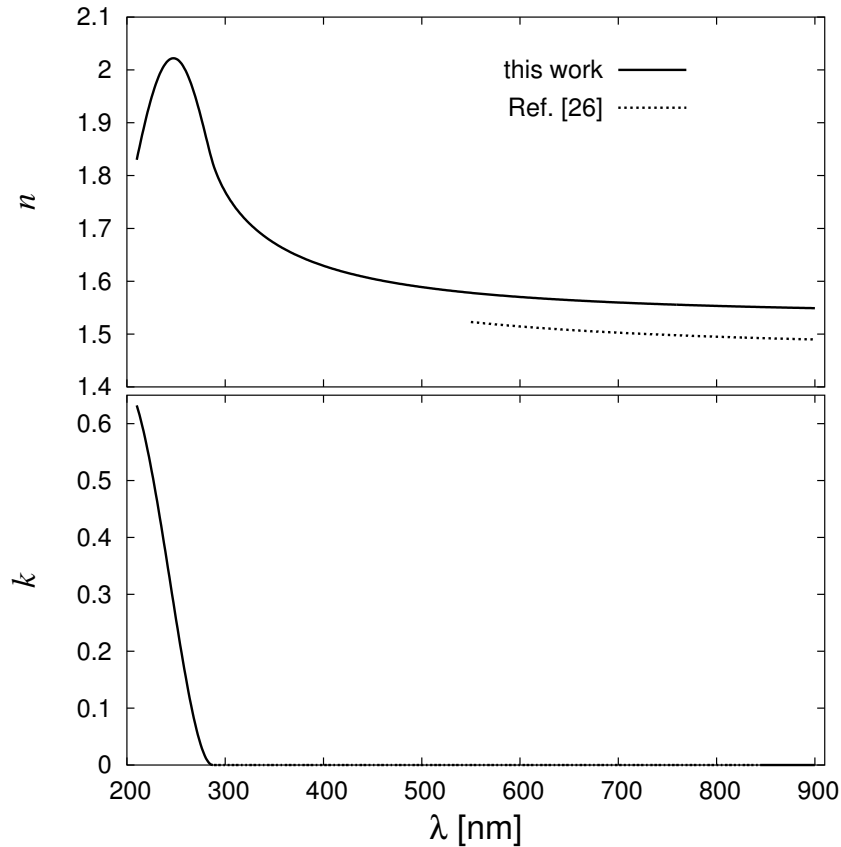


Fig. 7. The spectral dependences of the refractive index n and extinction coefficient k determined for the thermal oxide films (solid lines) and the spectral dependences of the refractive index of the films studied in Ref. [26] (dotted line).

values of the parameters describing the morphology of the film boundaries (this statement is especially valid for roughness). However, as mentioned above the application of this combination must be performed with a certain care. As for the statistical boundary roughness this statement is implied by the fact that the optical methods and AFM are sensitive to different intervals of the spatial frequencies of the harmonic components of roughness in principle. If the interval of the spatial frequencies of the rough boundary or surface is not simultaneously a subinterval of the intervals of both the methods, i. e. AFM and the optical methods, one cannot expect a good agreement between the results for the statistical quantities found using both the methods. Unfortunately, this fact occurs often in practice. The reasonable agreement can be expected only in the case that the entire interval of the spatial frequencies of the roughness lies within both the intervals of spatial frequency sensitivity of AFM and the combined optical method of VASE and spectrophotometry (e. g. spectroscopic reflectometry). The interval of sensitivity concerning the

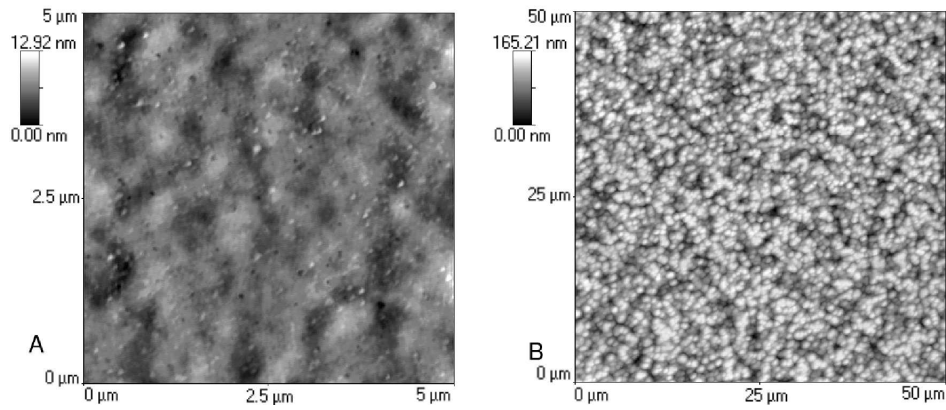


Fig. 8. The AFM images of the upper boundary of the thermal oxide film (A) and the corresponding rough GaAs surface after dissolution this film (B). The time of oxidation was of 6 hours.

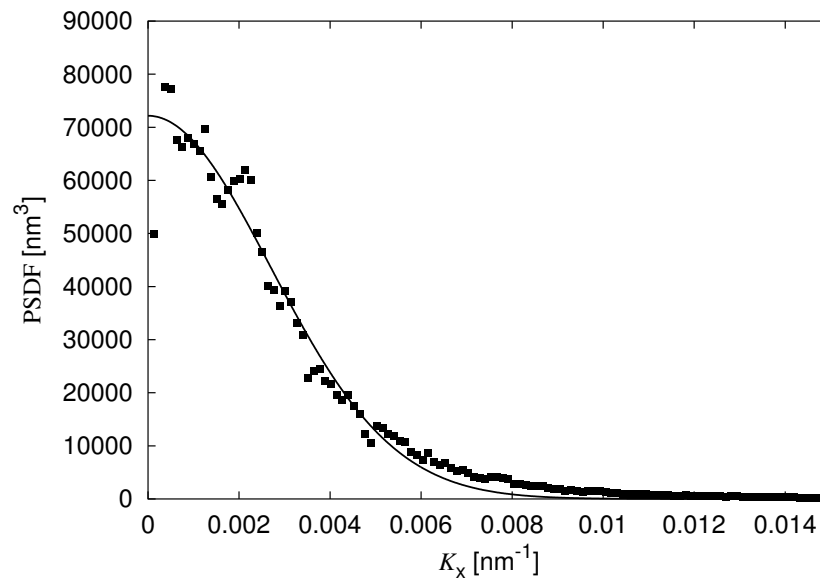


Fig. 9. The PSDF of the rough GaAs surface corresponding to the time of oxidation of 7 hours. Squares represent the values obtained by means of AFM, the solid line corresponds to the Gaussian fit.

spatial frequencies of statistical roughness corresponding to AFM is given by the diameter of the apex of the AFM tip employed in the microscope used and the length of the side of the scan performed (the scans are mostly formed by squares). The diameter of the apex determines the

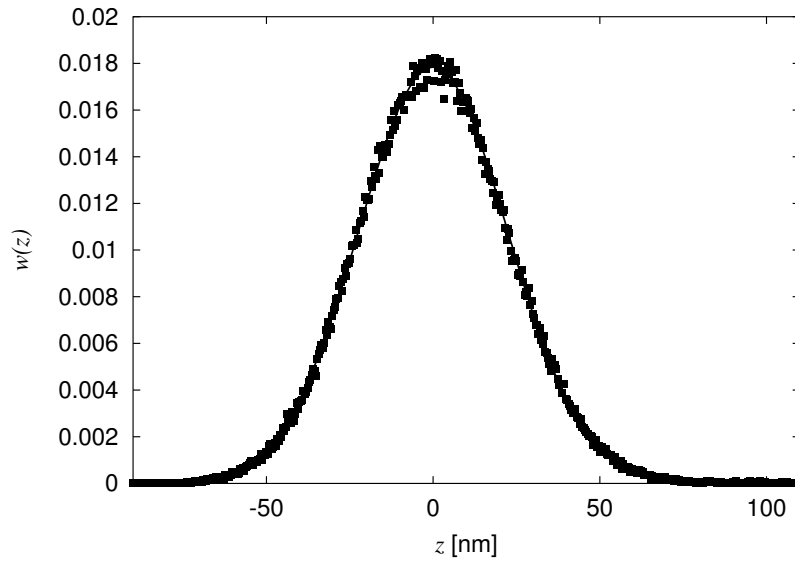


Fig. 10. The values $w(z)$ of the rough GaAs surface corresponding to the time of oxidation of 7 hours. Squares represent the values obtained by means of AFM, the solid line corresponds to the Gaussian fit.

highest limit and scan length determines the lowest limit of the interval of frequency sensitivity. In the case of the optical methods, e. g. VASE and spectroscopic reflectometry, it is more complicated to estimate the intervals of frequency sensitivity in practice. These intervals depend on several factors. For example, the intervals depend on the acceptance angles of the detectors employed in experimental arrangements serving for measurements of the optical quantities, spectral regions in which the optical measurements are performed and optical constants of the materials separated by the rough boundaries. Therefore, the estimation of the intervals of the frequency sensitivity must be performed individually for every optical method used to study the layered systems with the rough boundaries.

The fact discussed in the foregoing text of this section is probably one of the main reasons of the disagreement in AFM and optical values of the roughness parameters found for the upper boundaries of the titania film studied (see Table 1). The roughness of the upper boundaries of the columnar films is very fine (i. e. this is nanometric roughness) so that the AFM measurements performed with the usual tips cannot be perfectly reliable. The apex tip diameters are usually 20–50 nm and therefore the interval of the frequency sensitivity of usual AFM cannot include the entire interval of the spatial frequencies of the upper boundaries of the columnar films including the titania films under study. The lateral dimensions of the upper boundary roughness of these films are namely in values smaller or comparable with these diameter values. If the intervals of sensitivity of AFM and the optical methods are not identical or not containing the intervals of the spatial frequencies corresponding to the rough surfaces or boundaries studied the values of the statistical quantities determined using these methods can not be strictly correct. The corre-

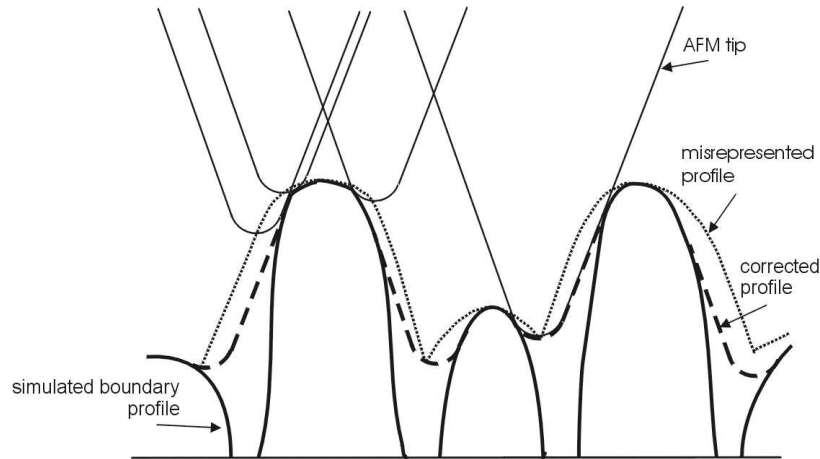


Fig. 11. Schematic diagram expressing the influence of the tip on measuring the profile of the upper boundary and improvement of this profile measured using the correcting procedure employed.

sponding errors in determining the roughness quantities are dependent, of course, on the relations between these intervals. This fact can be illustrated by means of the theoretical analysis of the AFM characterization of the boundary roughness of the upper boundaries of the columnar thin films presented in paper [15]. In this paper the simulation of the growth of the columnar thin films were carried out using the simple (2+1)-dimensional algorithm based on the Monte Carlo procedure (for details see paper [15]). In this way the rough upper boundaries of the columnar films could be determined theoretically. Furthermore, the AFM measurements of these rough boundaries were simulated for the tips with various apex diameters. In Fig. 11 a schematic diagram expressing the influence of the tip on measuring the profile of the upper boundary is shown. From this figure the misrepresentation of the real (correct) profile of the rough boundary caused by the finite dimensions of the used tip is evident (the misrepresented AFM profile is denoted as dilated profile in this figure). From Fig. 11 one can see that when the misrepresented (dilated) profile corresponding to the profile measured in practice is treated the strongly misrepresented values of the basic statistical quantities will be determined. This misrepresenting effect of the profile of the rough surface is called the convolution of the tip and surface. Therefore several algorithms were developed for reducing the influence of the tips on the AFM measurements of the fine randomly rough surfaces. The most known algorithm is the Villarrubia's one [27]. Using this Villarrubia's algorithm it is possible to correct the dilated profile as shown in Fig. 11 (the profile corrected by this algorithm is denoted as the reconstructed profile). One can see that using the Villarrubia's procedure it is not possible to correct the profile markedly (the same statement is valid for the other correcting procedures). This can be confirmed by the quantitative analysis performed in [13, 15]. Within this analysis several relations between linear dimensions of the tips and surfaces were considered (see Fig. 12). In Fig. 12 symbol z denotes the heights of irregularities and x represents the coordinate along the scan. All the profiles, i. e. simulated, dilated (misrepresented) and reconstructed, are shown for three differently rough surfaces owing to the

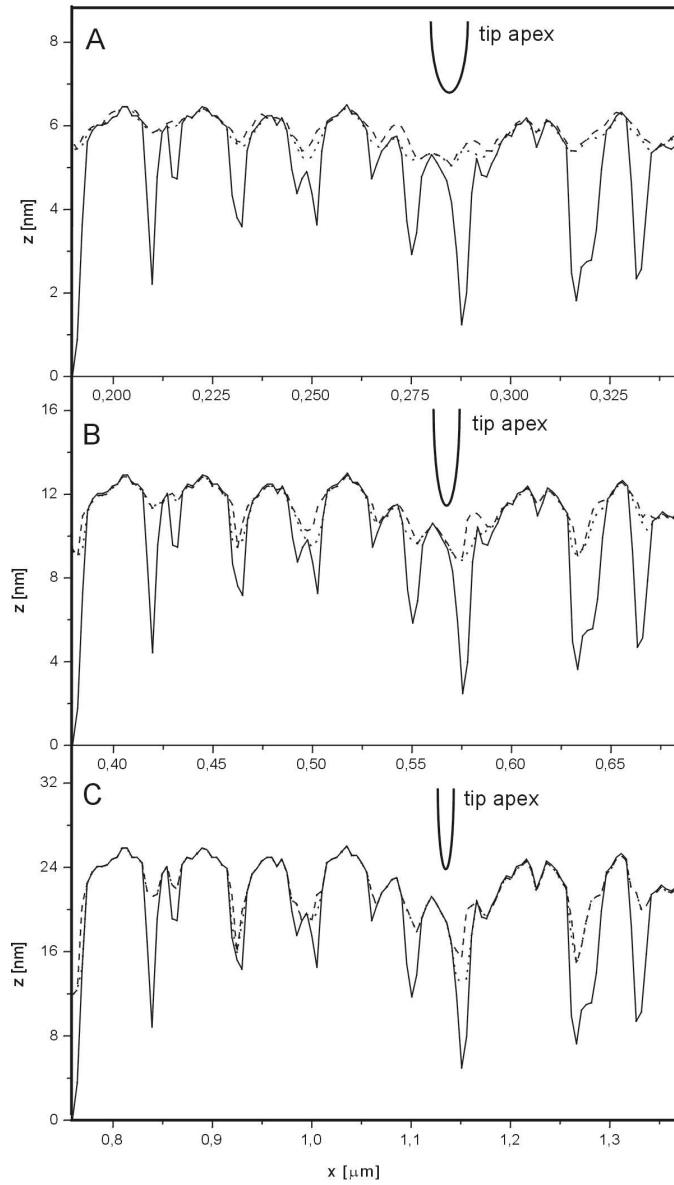


Fig. 12. Cross-sections of the three simulated upper boundaries of the columnar films A, B and C corresponding to the different relationships between the linear dimensions of tip and columns: — - simulated profile, - - - - misrepresented (measured) profile, - corrected profile. Note that the tip apexes appear to be parabolic ones because the scales on both the coordinate axes are different.

tips, i. e. the fine, medium and coarse surfaces are inspected owing to the tips. In this figure the tips are drawn in the corresponding scale (they do not exhibit the form of circles because of the different scales of the z and x axes). The rms values of the heights σ and the rms values of the angles of the slopes $\tan \alpha_0$ corresponding to the simulated, dilated and reconstructed surfaces for all the three cases are summarized in Table 4 (e. g. for the Gaussian rough surface holds that $\tan \alpha_0 = \sqrt{2}\sigma/T$). One can see that the values of both the roughness parameters are strongly misrepresented for both the dilated and reconstructed surface in comparison with the simulated (real) surface. The same conclusions were found for the other statistical quantities (e. g. for PSDF). Thus, the tip influence on the values of the basic statistical quantities characterizing the relatively fine rough surfaces is very strong. Moreover, it is evident that the correcting procedures such as the Villarrubia's procedure cannot correct these values in a substantial way. This means that the AFM analysis of the surfaces with fine roughness, i. e. with statistical roughness exhibiting very high spatial frequencies, gives considerably misrepresented results. In this case the fine rough surface exhibits the high spatial frequencies that are not contained within the sensitivity interval of AFM. This fact must be respected in the optical characterization of the optical properties of the layered systems with finely rough boundaries. Thus, the values of the statistical parameters determined for the titania films and other columnar thin films by the optical methods are evidently more correct than those determined using AFM because the fine roughness can be included into the formulae expressing the optical quantities in a relatively exact way (the same statement is true for the pm-Si:H films too). Using the detailed discussion one can even show that the optical values of the roughness parameters determined for the columnar films are very close to the true ones. Of course, if the layered systems exhibit the rough boundaries with sufficiently smaller spatial frequencies the AFM analysis of their boundaries will give relatively correct results that can be utilized for the optical characterization of such the systems with a high reliability. This statement is also supported by the values of σ and α_0 presented in Table 4. From this table it is evident that the coarser rough surface (sample C) is influenced by the convolution less than finer rough surfaces (see e. g. surface A). Thus, this coarser surface contains less number of the high frequencies that are not included in the interval sensitivity of the corresponding AFM tip.

It should be noted that the values of the autocorrelation length T corresponds to the spatial frequencies of the rough surfaces (see e. g. Ref. [15]). Smaller values of T correspond to the higher spatial frequencies while greater ones correspond to the lower spatial frequencies. Therefore one can expect that the values of σ and T determined using AFM for the thermal oxide films on GaAs are correct (compare Tables 1–3). Thus, the fixation of the T values determined with AFM within the optical analyses of these films is apparently reasonable.

6 Conclusion

In this paper the examples of the important combined methods usable for characterization of the optical properties of the thin films are presented. These methods are based on combining the optical methods, i. e. VASE and spectroscopic reflectometry, and AFM. It is shown that these methods can be classified into the two basic groups. The first group consists of the methods utilizing AFM as the checking method for confirming the values of the parameters characterizing morphology (in particular roughness) that are evaluated using the optical methods at charac-

Tab. 4. The rms values of the heights σ and slope angles α_0 (for details see the text).

boundary	α_0 [deg]	σ [nm]
A		
original	22.47	1.382
misrepresented	5.40	0.366
corrected	5.47	0.405
B		
original	22.47	2.763
misrepresented	8.414	0.999
corrected	9.387	1.210
C		
original	22.47	5.526
misrepresented	11.82	2.732
corrected	12.97	3.159

terizing the optical properties of rough layered systems (methods denoted as CM1). The two examples of the CM1 are presented in this paper. The first example concerns the optical analysis of the TiO₂ films and the latter example concerns the optical analysis of the hydrogenated polycrystalline Si films (pm-Si:H films). The methods of the latter group, i. e. the methods belonging to CM2, are illustrated using the complete characterization of the thin oxide films originating by thermal oxidation of GaAs. Within the latter group AFM is used to determining the values of some roughness parameters of the film boundaries that then are employed as the known values in the optical characterization of the rough thin films (of course, in principle AFM can be used to characterize parameters describing the other kinds of boundary morphology). In principle both the combined methods, i. e. the CM1 and CM2, can be used in the two modifications. The first modification employs the dispersion models whereas the latter one does not use these models (in this case the data treatment is performed individually in many wavelengths taking place in the spectral regions of interest). Furthermore, it is shown that the methods presented here are very efficient for the analysis of the complicated thin films existing in practice (the films studied here by the described methods exhibited very complicated structure with the various defects). In this paper the discussion of the correctness of the results achieved using the methods described is presented. The attention is especially devoted to the correctness of the results concerning the roughness parameters characterizing very fine rough boundaries. It is shown that the values of the statistical parameters of this fine roughness determined by AFM are strongly misrepresented and that their utilization in the combined methods is problematic. Moreover, it is presented that using the optical methods and AFM the same results can be achieved for the roughness parameters only when the intervals of the spatial frequencies of the rough surfaces are subintervals of the intervals in which the optical methods and AFM are sensitive to spatial frequencies.

Acknowledgement: This work was supported by Ministry of Education of the Czech Republic under contract MSM143100003 and by Ministry of Industry and Commerce of the Czech

Republic within the program TANDEM under Contract No. FT-TA/094.

References

- [1] R. M. A. Azzam, N. M. Bashara: *Ellipsometry and Polarized Light*, North-Holland, Amsterdam 1977
- [2] I. Ohlídal, D. Franta: *Ellipsometry of Thin Film Systems*, in *Progress in Optics*, vol. 41., ed. E. Wolf; Elsevier, Amsterdam 2000, pp. 181–282
- [3] K. Riedling: *Ellipsometry for Industrial Applications*, Springer, Wien 1988
- [4] I. Ohlídal, D. Franta, *Acta Phys. Slov.* **50** (2000) 489
- [5] D. Franta, I. Ohlídal, P. Klapetek, *Mikrochim. Acta* **132** (2000) 443
- [6] D. Franta, I. Ohlídal, P. Klapetek, P. Pokorný, *Surf. Interface Anal.* **34** (2002) 759
- [7] D. Franta, I. Ohlídal, *Acta Phys. Slov.* **50** (2000) 411
- [8] D. Franta, I. Ohlídal, P. Klapetek, P. Roca i Cabarrocas, *Thin Solid Films* **455–456** (2004) 399
- [9] D. Franta, I. Ohlídal, P. Klapetek, A. Montaigne Ramil, A. Bonanni, D. Stifter, H. Sitter, *Thin Solid Films* **468** (2004) 193
- [10] G. Atanasov, J. Turlo, J. K. Fu, Y. S. Dai, *Thin Solid Films* **342** (1999) 83
- [11] C. Ting, S. Chen, *J. Appl. Phys.* **88** (2000) 4628
- [12] P. Dumas, B. Bouffakhredine, C. Amra, O. Vatel, E. Andre, R. Galindo, F. Salvan, *Europhys. Lett.* **22** (1993) 717
- [13] P. Klapetek, I. Ohlídal, K. Navrátil, *Mikrochim. Acta* **147** (2004) 175
- [14] P. Klapetek, I. Ohlídal, A. Montaigne Ramil, A. Bonanni, D. Stifter, H. Sitter, *Jpn. J. Appl. Phys.* **42** (2003) 4706
- [15] P. Klapetek, I. Ohlídal, *Ultramicroscopy* **94** (2003) 19
- [16] B. Cappella, G. Dietler, *Surf. Sci. Rep.* **34** (1999) 1
- [17] D. Franta, I. Ohlídal, P. Klapetek, A. Montaigne Ramil, A. Bonanni, D. Stifter, H. Sitter, *J. Appl. Phys.* **92** (2002) 1873
- [18] D. Franta, I. Ohlídal, *J. Mod. Opt.* **45** (1998) 903
- [19] D. Franta, I. Ohlídal, M. Frumar, J. Jedelský, *Appl. Surf. Sci.* **212–213** (2003) 116
- [20] J. Tauc: in *Optical Properties of Solids*, ed. F. Abelès; North-Holland, Amsterdam 1972, p. 291
- [21] D. L. Wood, J. Tauc, *Phys. Rev. B* **5** (1972) 3144
- [22] C. M. Herzinger, B. Johs, W. A. McGahan, J. A. Woollam, W. Paulson, *J. Appl. Phys.* **83** (1998) 3323
- [23] D. Franta, I. Ohlídal, P. Klapetek, M. Ohlídal, *Surf. Interface Anal.* **32** (2001) 91
- [24] P. Klapetek, I. Ohlídal, D. Franta, P. Pokorný, M. Ohlídal, *Surf. Interface Anal.* **34** (2002) 559
- [25] D. Franta, I. Ohlídal, P. Klapetek, M. Ohlídal, *Surf. Interface Anal.* **36** (2004) 1203
- [26] I. Ohlídal, F. Vižďa, M. Ohlídal, *Opt. Eng.* **34** (1995) 1761
- [27] J. S. Villarrubia, *J. Res. Natl. Inst. Stand. Technol.* **102** (1997) 425